

Dynamical system approach and attracting manifolds in K - ε model of turbulent jet

D.V. Strunin

Abstract

We consider the K - ε model describing an expansion of a free turbulent jet. Due to the nonlinear nature of turbulent diffusion the turbulent area has a sharp boundary. We seek solutions for the energy, dissipation and momentum as power series in spatial coordinate across the jet with time-dependent coefficients. The coefficients obey a dynamical system with clearly identifiable slow and fast variables. The system is not in a standard form, which excludes rigorous methods of analysis such as centre manifold methods. We put forward a hypothesis that there exists an attracting invariant manifold for trajectories based on a few slow variables. The hypothesis is supported numerically.

1 The K - ε model of a turbulent jet

We consider the dynamics of a turbulent jet developing in an unbounded motionless fluid from an initially narrow plane layer. Statistically, the jet is uniform downstream, so that the ensemble-averaged turbulent energy, momentum and other characteristics depend only on the coordinate across (but not along) the jet and time.

The velocity shear between the jet and surrounding fluid generates kinetic energy of turbulent pulsations K . The turbulent volume expands and, in the long-term, the turbulent energy decays due to the geometric effect of expansion and the loss into heat caused by intersections of vortices. The latter effect is expressed by the energy dissipation rate ε .

The expansion is driven by the turbulent diffusion which is essentially nonlinear. Due to the nonlinearity there exists a sharp boundary—front—between the jet and

1991 *Mathematics Subject Classification* : 37L25, 37N10.

Key words and phrases : nonlinear diffusion, dynamical system, attractor.

surrounding fluid. This property is analogous to confinement of solutions of a single diffusion equation with the diffusion coefficient depending on the function of interest [1] (for other examples see, e.g. [2]). For example, the equation $\partial_t f = \partial_x (f \partial_x f)$ has the well-known similarity solution $f(x, t) = \alpha/t^{1/3} (1 - \beta x^2/t^{2/3})$, where α and β are constants. The point in space where $f(x, t)$ turns into zero defines the position of the front: $1 - \beta x^2/t^{2/3} = 0$ gives $x = h(t) = t^{1/3} \sqrt{\beta}$. Importantly, such a solution is an attractor for solutions evolving from different initial conditions.

For the turbulent jet, we have several coupled variables subject to nonlinear diffusion. Consider the K - ε model [3, 4] describing the dynamics of the turbulent kinetic energy K , its dissipation rate ε and momentum u :

$$\begin{aligned}\partial_t K &= \alpha_1 \partial_x \left(\frac{K^2}{\varepsilon} \partial_x K \right) + \alpha_2 \frac{K^2}{\varepsilon} (\partial_x u)^2 - \alpha_3 \varepsilon, \\ \partial_t \varepsilon &= \beta_1 \partial_x \left(\frac{K^2}{\varepsilon} \partial_x \varepsilon \right) + \beta_2 K (\partial_x u)^2 - \beta_3 \frac{\varepsilon^2}{K}, \\ \partial_t u &= \chi \partial_x \left(\frac{K^2}{\varepsilon} \partial_x u \right).\end{aligned}\tag{1}$$

The coordinate x is directed across the turbulent layer starting in its middle. The layer is infinite and uniform in the y and z directions. In (1) $\alpha_{1,2,3}$, $\beta_{1,2,3}$ and χ are non-dimensional constants. The system (1) is non-dimensional, obtained from the dimensional form by using some useful scales, for example, the average initial velocity across the jet, U , as the velocity scale; the initial width of the jet, $2h$, as the length scale; U^2 as the turbulent energy scale; U^3/h as the dissipation rate scale; and h/U as the time scale.

The initial profiles for K , ε and u across the turbulent layer are supposed to be dome-like and symmetric with respect to the middle of the layer. On the edge, or front, of the jet the functions of interest turn into zero and remain zero beyond the front.

2 Dynamical system approach

We look for solutions of (1) as power series in x :

$$\begin{aligned}K &= A(t) [1 - B_2(t)x^2 - B_4(t)x^4 - B_6(t)x^6 - \dots], \\ \varepsilon &= P(t) [1 - R_2(t)x^2 - R_4(t)x^4 - R_6(t)x^6 - \dots], \\ u &= M(t) [1 - N_2(t)x^2 - N_4(t)x^4 - N_6(t)x^6 - \dots].\end{aligned}\tag{2}$$

Here A , P and M are the values of the functions $K(x, t)$, $\varepsilon(x, t)$ and $u(x, t)$ in the middle of the layer, $x = 0$. The structure functions in the square brackets describe dome-like profiles descending to zero at some finite x , the coordinate of the front.

Substituting the series (2) into the dynamic equations (1) and collecting terms

with same powers of x gives the system of ODEs

$$\begin{aligned}
 \dot{A} &= -\alpha_1 \frac{2A^3 B_2}{P} - \alpha_3 P, \\
 \dot{P} &= -\beta_1 2A^2 R_2 - \beta_3 \frac{P^2}{A}, \\
 \dot{M} &= -\chi \frac{2A^2 M N_2}{P}, \\
 \dot{B}_2 &= -\alpha_1 \frac{10A^2 B_2^2}{P} + \alpha_3 \frac{P B_2}{A} + \alpha_1 \frac{6A^2 B_2 R_2}{P} + \alpha_1 \frac{12A^2 B_4}{P} \\
 &\quad - \alpha_2 \frac{4AM^2 N_2^2}{P} - \alpha_3 \frac{P R_2}{A}, \\
 \dot{R}_2 &= -\beta_1 \frac{12A^2 B_2 R_2}{P} + \beta_1 \frac{8A^2 R_2^2}{P} - \beta_3 \frac{P R_2}{A} + \beta_1 \frac{12A^2 R_4}{P} \\
 &\quad - \beta_2 \frac{4AM^2 N_2^2}{P} + \beta_3 \frac{P B_2}{A}, \\
 \dot{N}_2 &= -\chi \frac{12A^2 B_2 N_2}{P} + \chi \frac{2A^2 N_2^2}{P} + \chi \frac{6A^2 N_2 R_2}{P} + \chi \frac{12A^2 N_4}{P},
 \end{aligned} \tag{3}$$

$$\begin{aligned}
 \dot{B}_4 &= -\alpha_1 \frac{58A^2 B_2 B_4}{P} + \alpha_3 \frac{P B_4}{A} + \alpha_1 \frac{10A^2 B_2^3}{P} - \alpha_1 \frac{20A^2 B_2^2 R_2}{P} \\
 &\quad + \alpha_1 \frac{10A^2 B_2 R_2^2}{P} + \alpha_1 \frac{10A^2 B_2 R_4}{P} + \alpha_1 \frac{20A^2 B_4 R_2}{P} + \alpha_1 \frac{30A^2 B_6}{P} \\
 &\quad + \alpha_2 \frac{8AB_2 M^2 N_2^2}{P} - \alpha_2 \frac{4AM^2 N_2^2 R_2}{P} - \alpha_2 \frac{16AM^2 N_2 N_4}{P} - \alpha_3 \frac{P R_4}{A}, \\
 \dot{R}_4 &= -\beta_1 \frac{40A^2 B_2 R_4}{P} + \beta_1 \frac{2A^2 R_2 R_4}{P} - \beta_3 \frac{P R_4}{A} + \beta_1 \frac{10A^2 B_2^2 R_2}{P} \\
 &\quad - \beta_1 \frac{20A^2 B_2 R_2^2}{P} - \beta_1 \frac{20A^2 B_4 R_2}{P} + \beta_1 \frac{10A^2 R_2^3}{P} + \beta_1 \frac{30A^2 R_2 R_4}{P} \\
 &\quad + \beta_1 \frac{30A^2 R_6}{P} + \beta_2 \frac{4AB_2 M^2 N_2^2}{P} - \beta_2 \frac{16AM^2 N_2 N_4}{P} + \beta_3 \frac{B_2^2 P}{A} \\
 &\quad - \beta_3 \frac{2B_2 P R_2}{A} + \beta_3 \frac{B_4 P}{A} + \beta_3 \frac{P R_2^2}{A}, \\
 \dot{N}_4 &= -\chi \frac{40A^2 B_2 N_4}{P} + \chi \frac{2A^2 N_2 N_4}{P} + \chi \frac{10A^2 B_2^2 N_2}{P} - \chi \frac{20A^2 B_2 N_2 R_2}{P} \\
 &\quad - \chi \frac{20A^2 B_4 N_2}{P} + \chi \frac{10A^2 N_2 R_2^2}{P} + \chi \frac{10A^2 N_2 R_4}{P} + \chi \frac{20A^2 N_4 R_2}{P} \\
 &\quad + \chi \frac{30A^2 N_6}{P}, \\
 &\dots
 \end{aligned} \tag{4}$$

A solution consistent with physics of diffusion can only be obtained if the system (3)–(4) is coupled with the explicit requirement that the fronts of the turbulent

energy, dissipation rate and velocity coincide. As we saw in the experiments, in absence of this requirement the fronts diverge from each other, which is unphysical.

Thus, K , ε and u turn into zero at the same point $x = h(t)$. Taking into account the terms up to the fourth-order in the power series (2) we require

$$\begin{aligned} 1 - B_2 h^2 - B_4 h^4 &= 0, \\ 1 - R_2 h^2 - R_4 h^4 &= 0, \\ 1 - N_2 h^2 - N_4 h^4 &= 0. \end{aligned} \quad (5)$$

The front equations (5) are complemented by the truncated dynamic equations (3),

$$\begin{aligned} \dot{A} &= -\alpha_1 \frac{2A^3 B_2}{P} - \alpha_3 P, \\ \dot{P} &= -\beta_1 2A^2 R_2 - \beta_3 \frac{P^2}{A}, \\ \dot{M} &= -\chi \frac{2A^2 M N_2}{P}, \\ \dot{B}_2 &= -\alpha_1 \frac{10A^2 B_2^2}{P} + \alpha_3 \frac{P B_2}{A} + \alpha_1 \frac{6A^2 B_2 R_2}{P} + \alpha_1 \frac{12A^2 B_4}{P} \\ &\quad - \alpha_2 \frac{4AM^2 N_2^2}{P} - \alpha_3 \frac{P R_2}{A}, \\ \dot{R}_2 &= \beta_1 \frac{8A^2 R_2^2}{P} - \beta_3 \frac{P R_2}{A} - \beta_1 \frac{12A^2 B_2 R_2}{P} + \beta_1 \frac{12A^2 R_4}{P} \\ &\quad - \beta_2 \frac{4AM^2 N_2^2}{P} + \beta_3 \frac{P B_2}{A}, \\ \dot{N}_2 &= \chi \frac{2A^2 N_2^2}{P} - \chi \frac{12A^2 B_2 N_2}{P} + \chi \frac{6A^2 N_2 R_2}{P} + \chi \frac{12A^2 N_4}{P}, \\ \dot{B}_4 &= -\alpha_1 \frac{58A^2 B_2 B_4}{P} + \alpha_3 \frac{P B_4}{A} + \alpha_1 \frac{10A^2 B_2^3}{P} - \alpha_1 \frac{20A^2 B_2^2 R_2}{P} \\ &\quad + \alpha_1 \frac{10A^2 B_2 R_2^2}{P} + \alpha_1 \frac{10A^2 B_2 R_4}{P} + \alpha_1 \frac{20A^2 B_4 R_2}{P} + \alpha_1 \frac{30A^2 B_6}{P} \\ &\quad + \alpha_2 \frac{8AM^2 N_2^2 B_2}{P} - \alpha_2 \frac{4AM^2 N_2^2 R_2}{P} - \alpha_2 \frac{16AM^2 N_2 N_4}{P} - \alpha_3 \frac{P^2 R_4}{AP}. \end{aligned} \quad (6)$$

The system (5)–(6) contains 10 equations with respect to 10 unknowns: A , P , M , B_2 , R_2 , N_2 , B_4 , R_4 , N_4 and h , all depending on t .

Introduce the new time by

$$\frac{d}{(A^2 B_2 / P) dt} = \frac{d}{d\tau} \equiv ()' \quad (7)$$

and divide (6) by $A^2 B_2 / P$. This conveniently converts (6) to the form with linear

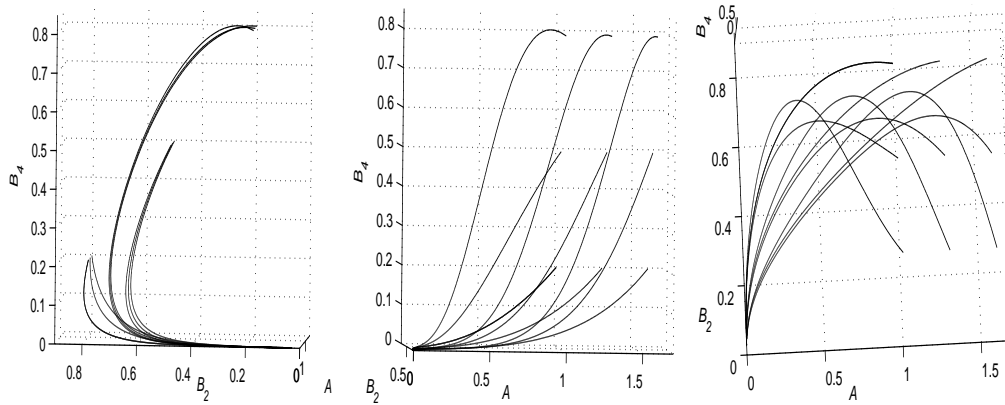


Figure 1: Trajectories (different views) in the space of the energy variables.

terms:

$$\begin{aligned}
 A' &= -\alpha_1 2A - \alpha_3 \frac{P^2}{A^2 B_2}, \\
 P' &= -\beta_1 \frac{2R_2 P}{B_2} - \beta_3 \frac{P^3}{A^3 B_2}, \\
 M' &= -\chi \frac{2MN_2}{B_2}, \\
 B_2' &= -\alpha_1 10B_2 + \alpha_3 \frac{P^2}{A^3} + \alpha_1 6R_2 + \alpha_1 \frac{12B_4}{B_2} \\
 &\quad - \alpha_2 \frac{4M^2 N_2^2}{AB_2} - \alpha_3 \frac{P^2 R_2}{A^3 B_2}, \\
 R_2' &= -\beta_1 12R_2 + \beta_1 \frac{8R_2^2}{B_2} - \beta_3 \frac{P^2 R_2}{A^3 B_2} + \beta_1 \frac{12R_4}{B_2} \\
 &\quad - \beta_2 \frac{4M^2 N_2^2}{AB_2} + \beta_3 \frac{P^2}{A^3}, \\
 N_2' &= -\chi 12N_2 + \chi \frac{2N_2^2}{B_2} + \chi \frac{6N_2 R_2}{B_2} + \chi \frac{12N_4}{B_2}, \\
 B_4' &= -\alpha_1 58B_4 + \alpha_3 \frac{P^2 B_4}{A^3 B_2} + \alpha_1 10B_2^2 - \alpha_1 20B_2 R_2 \\
 &\quad + \alpha_1 10R_2^2 + \alpha_1 10R_4 + \alpha_1 \frac{20B_4 R_2}{B_2} + \alpha_1 \frac{30B_6}{B_2} \\
 &\quad + \alpha_2 \frac{8M^2 N_2^2}{A} - \alpha_2 \frac{4M^2 N_2^2 R_2}{AB_2} - \alpha_2 \frac{16M^2 N_2 N_4}{AB_2} - \alpha_3 \frac{P^2 R_4}{A^3 B_2}.
 \end{aligned} \tag{8}$$

Numerical solutions of the system (5), (8) are displayed in Fig. 1–3. We used $\alpha_1 = 0.09$, $\alpha_2 = 0.09$, $\alpha_3 = 1$, $\beta_1 = 0.07$, $\beta_2 = 0.13$, $\beta_3 = 1.92$, $\chi = 0.09$.

One can easily distinguish fast and slow variables. See that the amplitudes A and P decay rapidly in comparison to B_2 and R_2 ; this decay is largely due to

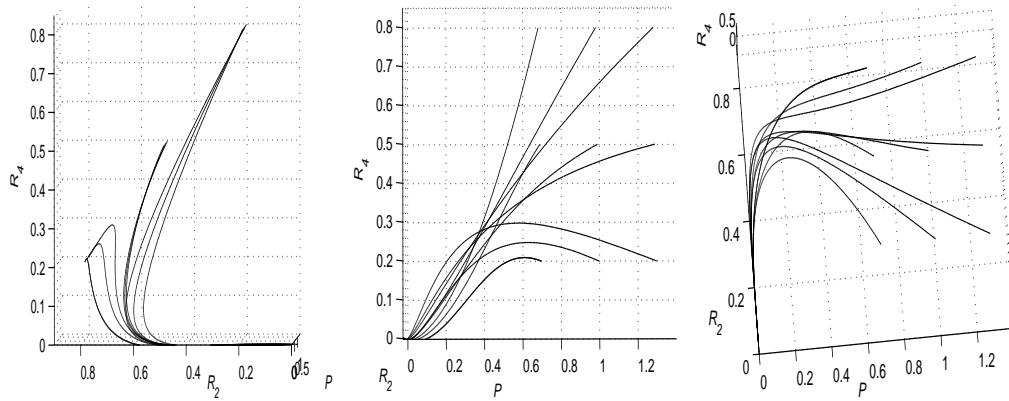


Figure 2: Trajectories (different views) in the space of the dissipation-rate variables.

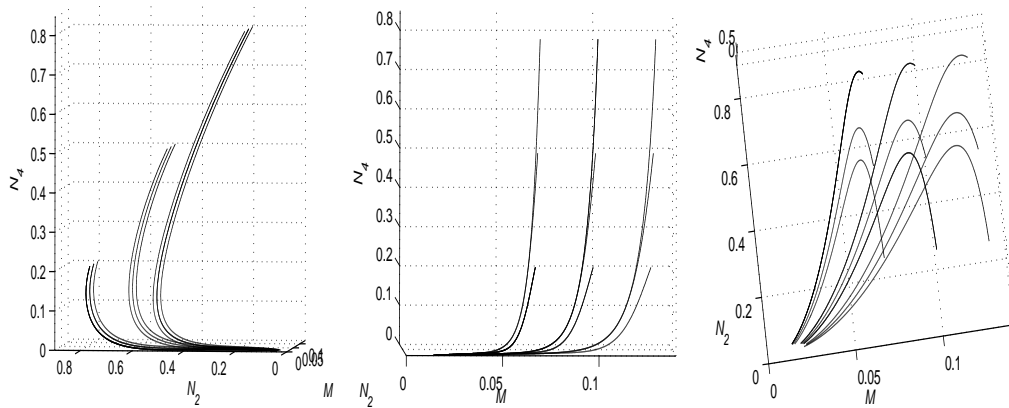


Figure 3: Trajectories (different views) in the space of the velocity variables.

the terms with α_3 and β_3 , that is the terms associated with the turbulent energy dissipation rate. The velocity amplitude, M , in comparison to N_2 , decays not so rapidly. The variables B_4 , R_4 and N_4 (and higher-order variables) too decay rapidly when compared to B_2 , R_2 and N_2 . Thus, the variables B_2 , R_2 and N_2 are slow and variables B_i , R_i and N_i for $i = 4, 6, \dots$ are fast.

It is convenient to transform the system to a form close to standard, which is the one comprising a few dynamic equations for slow variables followed by an infinite sequence of dynamic equations for rapid variables. This can be done when we notice that, except in the amplitude equations (8) the variables A , P and M appear in the right-hand sides only in combinations P^2/A^3 and A/M^2 . We anticipate and later confirm that, despite P and A change rapidly, those ratios are slow. We define

$$E = \frac{P^2}{A^3}, \quad S = \frac{A}{M^2}. \tag{9}$$

Differentiating (9) and using the derivatives A' , P' and M' from (8) we deduce the dynamic equations for E and S . Also, we add the dynamic equation for N_4 so that all the 4th-order coefficients, B_4 , R_4 and N_4 , now evolve according to their

respective dynamic laws. As a result, we get the equations

$$\begin{aligned}
 S' &= -\alpha_1 2S - \alpha_3 \frac{ES}{B_2} + \chi^4 \frac{SN_2}{B_2}, \\
 E' &= -\beta_1 4 \frac{R_2 E}{B_2} + \alpha_1 6E + (3\alpha_3 - 2\beta_3) \frac{E^2}{B_2}, \\
 B_2' &= -\alpha_1 10B_2 + \alpha_3 E + \alpha_1 6R_2 + \alpha_1 \frac{12B_4}{B_2} \\
 &\quad - \alpha_2 \frac{4N_2^2}{SB_2} - \alpha_3 \frac{ER_2}{B_2}, \\
 R_2' &= -\beta_1 12R_2 + \beta_1 \frac{8R_2^2}{B_2} + \beta_3 \frac{ER_2}{B_2} + \beta_1 \frac{12R_4}{B_2} \\
 &\quad - \beta_2 \frac{4N_2^2}{SB_2} + \beta_3 E - \beta_3 \frac{2ER_2}{B_2}, \\
 N_2' &= -\chi 12N_2 + \chi \frac{2N_2^2}{B_2} + \chi \frac{6N_2 R_2}{B_2} + \chi \frac{12N_4}{B_2}, \\
 B_4' &= -\alpha_1 58B_4 + \alpha_3 \frac{EB_4}{B_2} + \alpha_1 10B_2^2 - \alpha_1 20B_2 R_2 \\
 &\quad + \alpha_1 10R_2^2 + \alpha_1 10R_4 + \alpha_1 \frac{20B_4 R_2}{B_2} + \alpha_1 \frac{30B_6}{B_2} \\
 &\quad + \alpha_2 \frac{8N_2^2}{S} - \alpha_2 \frac{4N_2^2 R_2}{SB_2} - \alpha_2 \frac{16N_2 N_4}{SB_2} - \alpha_3 \frac{ER_4}{B_2}, \\
 R_4' &= -\beta_1 40R_4 + \beta_1 2 \frac{R_2 R_4}{B_2} + \beta_3 \frac{ER_4}{B_2} + \beta_1 10B_2 R_2 - 20\beta_1 R_2^2 \\
 &\quad - \beta_1 20 \frac{R_2 B_4}{B_2} + \beta_1 10 \frac{R_2^3}{B_2} + \beta_1 30 \frac{R_2 R_4}{B_2} + \beta_1 30 \frac{R_6}{B_2} \\
 &\quad + \beta_2 4 \frac{N_2^2}{S} - \beta_2 16 \frac{N_2 N_4}{SB_2} + \beta_3 EB_2 - \beta_3 2ER_2 \\
 &\quad + \beta_3 \frac{EB_4}{B_2} + \beta_3 \frac{ER_2^2}{B_2} - \beta_3 2 \frac{ER_4}{B_2}, \\
 N_4' &= -\chi 40N_4 + \chi 2 \frac{N_2 N_4}{B_2} + \chi 10B_2 N_2 - \chi 20N_2 R_2 \\
 &\quad - \chi 20 \frac{N_2 B_4}{B_2} + \chi 10 \frac{N_2 R_2^2}{B_2} + \chi 10 \frac{N_2 R_4}{B_2} + \chi 20 \frac{R_2 N_4}{B_2}.
 \end{aligned} \tag{10}$$

The dynamical system (10) is complemented to the closed form by the front equations

$$\begin{aligned}
 1 - B_2 h^2 - B_4 h^4 - B_6 h^6 &= 0, \\
 1 - R_2 h^2 - R_4 h^4 - R_6 h^6 &= 0, \\
 1 - N_2 h^2 - N_4 h^4 &= 0.
 \end{aligned} \tag{11}$$

That the variables E , S and B_2 are indeed slow is demonstrated in Fig. 4. It shows that none of these variables decays faster than the other two.

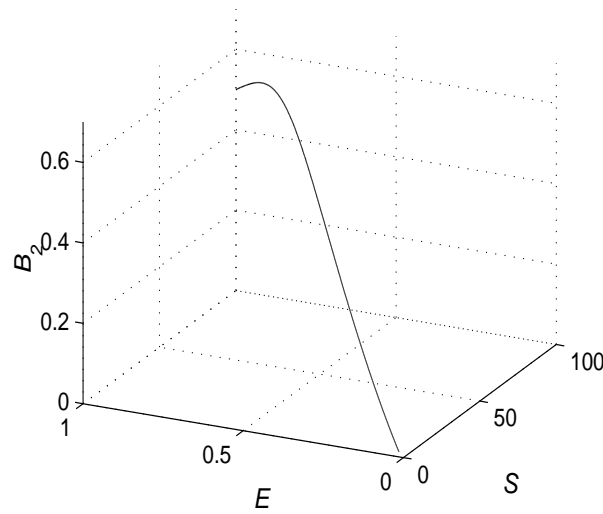


Figure 4: The behaviour of the slow variables.

Notice a spectral gap between the linear decay rates in (10) (and of course in (8)): the coefficient at B_4 , $(-58\alpha_1)$, is $5 \div 6$ times larger than the coefficient at B_2 , $(-10\alpha_1)$, at R_2 , $(-12\beta_1)$ and at N_2 , (-12χ) .

The numerical experiments show that the linear terms dominate on early stages of the dynamics. Hence, the fast variables quickly drop to levels where the linear terms are small enough to become of the same order as nonlinear.

3 Attracting manifolds: examples

This resembles a mechanism typical for centre manifolds and invariant manifolds. The centre manifold in an attractor for trajectories of a dynamical system where some (slow) variables have zero linear decay rates, while the other (fast) variables have negative linear decay rates [5]. We illustrate this by a simple example from [6]:

$$\begin{aligned} \dot{x} &= -px - xy, \\ \dot{y} &= -y + x^2 - 2y^2. \end{aligned} \tag{12}$$

If $p = 0$ we have a standard centre manifold case, and the attractor for all trajectories is

$$y = x^2. \tag{13}$$

This is also an exact solution of (12) (with x evolving according to $\dot{x} = -x^3$). Generally, any trajectory is asymptotically representable as power series in x with the leading term given by (13). Driven by the linear term $(-y)$, a trajectory quickly falls onto the manifold (13), on which the nonlinear term x^2 in (12) is comparable to the linear term $(-y)$. On the manifold the variable y depends on t only via x .

When p is positive but relatively small, the attracting manifold can be found as a perturbation of (13). This case is similar to our situation in (10).

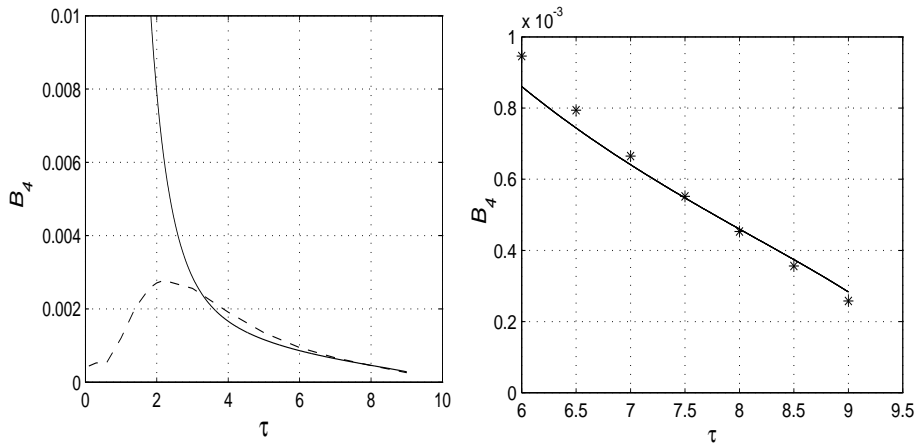


Figure 5: Actual behaviour of B_4 (solid line) and its projection onto the attractor. End part of the curve is zoomed.

Note that in the unperturbed case $p = 0$ the attractor (13) can be obtained by simply replacing the time derivative \dot{y} by zero: $0 = -y + x^2 - 2y^2$ giving $y = x^2 + o(x^2) \rightarrow x^2$ when $x \rightarrow 0$.

If $p > 0$, this rule does not apply and the derivative \dot{y} must be taken into account in order to get correct expression for the leading term of the attracting manifold. As an elementary example consider the purely linear system $\dot{x} = -px$, $\dot{y} = -y + x$, from where $x(t) = x(0)e^{-pt}$ and $y(t) = ae^{-t} + be^{-pt} \rightarrow be^{-pt}$ when $t \gg 1$. From the dynamic equation $-pb = -b + x(0)$ we find $b = x(0)/(1 - p)$, and therefore the attractor is $y \rightarrow [x(0)e^{-pt}]/(1 - p) = x/(1 - p)$. Apparently if we replace \dot{y} by zero in the dynamic equation, we get an incorrect form of the attractor: $y = x$. However, this is almost a correct answer when p is small enough. The greater the spectral gap between the linear decay rate 1 of y and p of x , the better the approximation $y = x$ of the actual attractor.

4 Attractor for the turbulent jet

In this section we exercise a similar trick in our turbulence problem aiming to find an approximate form of the attractor. In (10)–(11) we replace by zeroes the time derivatives in the dynamic equations for B_4 , R_4 and N_4 . This gives 6 algebraic equations to determine the 5 variables B_4 , R_4 , N_4 , B_6 , R_6 and h in terms of the slow variables E , S , B_2 , R_2 and N_2 . The algebraic equations are easily solvable numerically.

We compare two typical trajectories: one obtained from the full system (10)–(11) and the other obtained using the algebraic system as a source of the fast variable values in terms of the slow ones. The values of the slow variables in the latter case are taken the same as in the solution of the full system. The latter trajectory, therefore, represents an orthogonal projection of the actual trajectory onto a manifold which we hope can be a useful approximation of the attractor.

The comparison is shown in Fig. 5, 6, 7. For the energy and dissipation rate

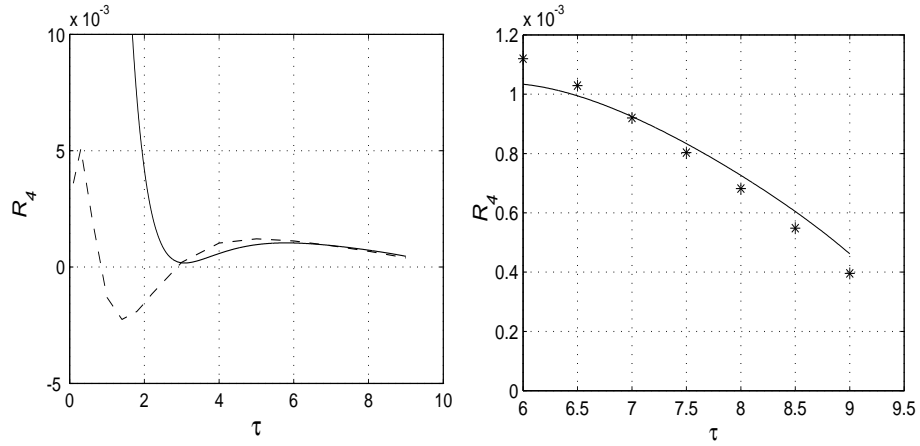


Figure 6: Actual behaviour of R_4 (solid line) and its projection.

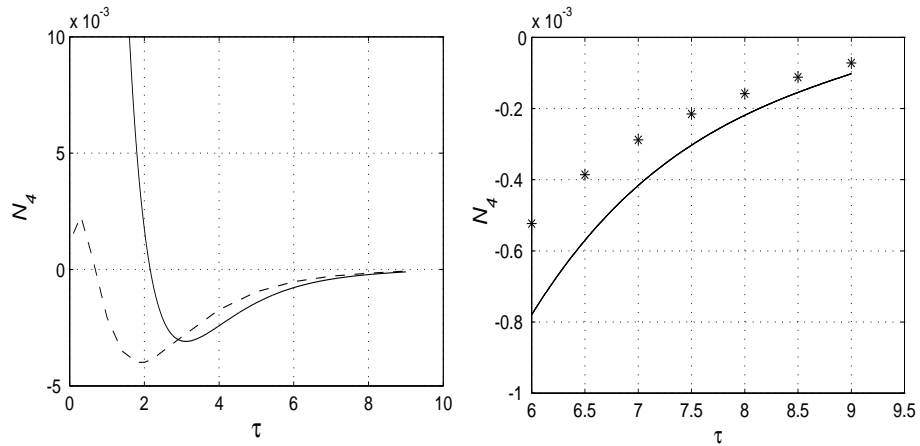


Figure 7: Actual behaviour of N_4 (solid line) and its projection.

variables the curves become very close at large times. For the velocity variables the curves are also close although to a lesser extent. Overall, the approach gives a reasonably accurate approximation.

5 Conclusions

We analyzed the $K-\varepsilon$ model of expanding turbulence shaped as a plane jet. Profiles of energy, dissipation rate and velocity across the jet are sought in the form of power series. The approach allows to naturally define the position of the front of turbulence. The series coefficients satisfy a nonlinear dynamical system with a few slow variables. Based on these variables, we approximately found an attractor in the form of a system of algebraic equations linking fast and slow variables:

$$\begin{aligned}
1 - B_2 h^2 - B_4 h^4 - B_6 h^6 &= 0, \\
1 - R_2 h^2 - R_4 h^4 - R_6 h^6 &= 0, \\
1 - N_2 h^2 - N_4 h^4 &= 0, \\
0 &= -\alpha_1 58 B_4 + \alpha_3 \frac{E B_4}{B_2} + \alpha_1 10 B_2^2 - \alpha_1 20 B_2 R_2 \\
&\quad + \alpha_1 10 R_2^2 + \alpha_1 10 R_4 + \alpha_1 \frac{20 B_4 R_2}{B_2} + \alpha_1 \frac{30 B_6}{B_2} \\
&\quad + \alpha_2 \frac{8 N_2^2}{S} - \alpha_2 \frac{4 N_2^2 R_2}{S B_2} - \alpha_2 \frac{16 N_2 N_4}{S B_2} - \alpha_3 \frac{E R_4}{B_2}, \\
0 &= -\beta_1 40 R_4 + \beta_1 2 \frac{R_2 R_4}{B_2} + \beta_3 \frac{E R_4}{B_2} + \beta_1 10 B_2 R_2 - 20 \beta_1 R_2^2 \\
&\quad - \beta_1 20 \frac{R_2 B_4}{B_2} + \beta_1 10 \frac{R_2^3}{B_2} + \beta_1 30 \frac{R_2 R_4}{B_2} + \beta_1 30 \frac{R_6}{B_2} \\
&\quad + \beta_2 4 \frac{N_2^2}{S} - \beta_2 16 \frac{N_2 N_4}{S B_2} + \beta_3 E B_2 - \beta_3 2 E R_2 \\
&\quad + \beta_3 \frac{E B_4}{B_2} + \beta_3 \frac{E R_2^2}{B_2} - \beta_3 2 \frac{E R_4}{B_2}, \\
0 &= -\chi 40 N_4 + \chi 2 \frac{N_2 N_4}{B_2} + \chi 10 B_2 N_2 - \chi 20 N_2 R_2 \\
&\quad - \chi 20 \frac{N_2 B_4}{B_2} + \chi 10 \frac{N_2 R_2^2}{B_2} + \chi 10 \frac{N_2 R_4}{B_2} + \chi 20 \frac{R_2 N_4}{B_2}.
\end{aligned}$$

A satisfactory agreement between the actual trajectories and their projections onto the attractor is demonstrated.

References

- [1] Ya.B. Zel'dovich and A.S. Kompaneets, On the theory of heat propagation for temperature dependent thermal conductivity. *Collection Commemorating the 70th Anniversary of A.F. Joffe, Izv. Akad. Nauk SSSR*, 1950.
- [2] A.D. Polyagin and V.F. Zaitsev, *Handbook of nonlinear partial differential equations*, Chapman and Hall/CRC, 2004, 814 pp.
- [3] B.E. Launder, G.J. Reece and W. Rodi, Progress in the development of a Reynolds-stress turbulence closure, *J. Fluid Mech.*, Vol. 68 (1975) pp. 537–566.
- [4] K. Hanjalic and B.E. Launder, A Reynolds stress model of turbulence and its applications to thin shear flows, *J. Fluid Mech.*, Vol. 52 (1972) pp. 609–638.
- [5] J. Carr, Applications of centre manifold theory, *Applied Mathematical Sciences*, Vol. 35, Springer-Verlag, 1981.

- [6] A.J. Roberts, Appropriate initial conditions for asymptotic descriptions of the long term evolution of dynamical systems, *J. Austral. Math. Soc. Ser. B*, Vol. 31 (1989) pp. 48–75.

Department of Mathematics and Computing
University of Southern Queensland
Toowoomba, QLD 4350, Australia
e-mail: strunin@usq.edu.au